Grid connected converters as reactive power ancillary service providers: Technical analysis for minimum required DC-link voltage

M. Merai, M.W. Naouar, I. Slama-Belkhodja, Eric Monmasson

▶ **To cite this version:**

M. Merai, M.W. Naouar, I. Slama-Belkhodja, Eric Monmasson. Grid connected converters as reactive power ancillary service providers: Technical analysis for minimum required DC-link voltage. Mathematics and Computers in Simulation, 2019, 158, pp.344-354. 10.1016/j.matcom.2018.09.016 . hal-03271461

HAL Id: hal-03271461
https://hal.science/hal-03271461

Submitted on 29 Jun 2021

HAL is a multi-disciplinary open access archive for the deposit and dissemination of scientific research documents, whether they are published or not. The documents may come from teaching and research institutions in France or abroad, or from public or private research centers.

L'archive ouverte pluridisciplinaire **HAL**, est destinée au dépôt et à la diffusion de documents scientifiques de niveau recherche, publiés ou non, émanant des établissements d'enseignement et de recherche français ou étrangers, des laboratoires publics ou privés.

Version of Record: https://www.sciencedirect.com/science/article/pii/S0378475418302489
Manuscript_8e4667be9717a64e8a2c75b16e187223

Grid Connected Converters as Reactive Power Ancillary Service Providers: Technical Analysis for Minimum required DC-Link Voltage

M. Merai[a], M. W. Naouar[b], I. Slama-Belkhodja[c] and E. Monmasson[d]

[a,b,c] Université de Tunis El Manar, Ecole Nationale d'Ingénieurs de Tunis, LR11ES15 Laboratoire de Systèmes Electriques, 1002, Tunis, Tunisie, Tunisia.
[b] SATIE-IUP GEII, rue d'Eragny, 95031 Cergy Pontoise, France.
e-mail: meriem.merai@enit.utm.tn[a], wissem.naouar@enit.utm.tn[b], ilhem.slamabelkhodja@enit.utm.tn[c], eric.monmasson@u-cergy.fr[d]

Abstract

Providing solutions for reactive power compensation next to reactive loads is beneficial for the efficiency of the overall grid system. The main reactive power compensation solutions are based on passive VAR generators (like capacitor banks) or active VAR generators (like static VAR generators). Extra use of VAR generators can be avoided by providing reactive power through renewable energy systems or loads, which are connected to the grid through *Grid connected Converters* (GcCs). In fact, GcCs can be controlled so that, in addition to their main control task, they realize an additional reactive power ancillary service. In this context, this paper investigates the achievement of reactive power ancillary service using three-phase GcCs and presents a detailed analysis regarding the determination of the minimal required DC-link voltage level for proper operation of GcCs as reactive power ancillary service providers. This analyse is done under both steady-state and transient conditions. Several simulation and experimental results are presented to confirm the validity of the obtained analytical results.

Keywords: Reactive power compensation, Grid connected Converters, DC-link voltage

1. Introduction

Reactive power compensation remains as an important technical challenge in the grid system for the reduction of the power transmission losses, the increase of the power transmission capabilities and the reduction of grid voltage dips [1]. To provide reactive power, passive and/or active solutions are generally used. In regard to passive solutions, capacitor banks are commonly employed. The use of this solution requires appropriate location and sizing of capacitor bank values. The main issue of this passive solution is the resonance problem that may occur when the capacitor bank is associated to inductive elements [2]. A more efficient and reliable solution for reactive power compensation can be achieved through dynamic VAR compensators like static VAR generators (SVGs) [3]. This kind of solution provides several advantages, such as dynamic and wide range of reactive power compensation in addition to accurate and reliable correction of the displacement power factor (DPF).

A key concern during the last years was the integration of renewable energy resources in the grid system. In fact, the fossil energy crisis and unsecured nuclear energy has motivated developed countries to enhance renewable technologies with the aim of more efficient and competitive power generation and control. Renewable energy resources are generally interfaced to the grid system through DC/AC grid connected inverters. Given that renewable energy resources are generally close to the point of power consumption, they can be used as reactive power ancillary service provider thanks to the flexibility of the related grid connected inverters [4-6]. On the other hand, with the reduced cost and enhanced reliability of power electronic converters, AC/DC grid connected rectifiers are more and more used to interface between some loads and the grid. Grid connected rectifiers use a power circuit similar to that of the grid connected inverter systems, but with the difference of power flow direction that becomes from the grid to the DC side. Therefore, they can also realize the same reactive power ancillary service using the same control as that developed for the grid connected inverter systems [5].

This paper focuses on the control of three-phase Grid connected Converters (GcCs) (*i.e.* Grid connected inverters or rectifiers) as reactive power ancillary service providers. The control of GcCs is generally based on two control loops: 1) an internal current control loop that ensures a decoupled control of active and reactive powers and 2) an external DC-link voltage control loop aimed to keep the level of the DC side voltage constant and equal to a predefined reference [9]. To ensure proper operation of GcCs as VAR generators and under both steady-state and transient conditions, the DC-link voltage must be selected enough high. On the other hand, a large increase of the DC-link voltage will lead to higher power losses, higher grid current THD and higher DC-link capacitor cost. Despite the fact that the selection of the DC-link voltage is very important for the considered application, there is a luck of related discussions with detailed analyse in previous publications [10]. In view of

© 2018 published by Elsevier. This manuscript is made available under the Elsevier user license
https://www.elsevier.com/open-access/userlicense/1.0/

this, this paper presents a detailed technical analysis for the determination of the minimum required DC-link voltage level. For this, the factors that must be considered in the selection of the DC-link voltage level are firstly identified. Then, a systematic and simplified approach that allows an adequate selection of the DC-link voltage level is presented.

The rest of the paper is organized as follows. Section 2 presents the modeling and control of a three-phase GcCs with reactive power ancillary service. Then, a detailed technical analysis for minimum required DC-link voltage selection is presented in section 3. After that, section 4 presents and discusses the obtained experimental results. Finally, the last section summarizes the main conclusions of this work.

2. Modeling and control of Three-phase GcC with reactive power ancillary srevice

2.1. Modeling

The power circuit of a three-phase GcC that operates as reactive power ancillary service provider is presented on Fig.1.a. In this figure, $V_{g(a,b,c)}$ are the grid voltages at the point of common coupling (PCC), $i_{L(a,b,c)}$ are currents consumed by local loads, $i_{g(a,b,c)}$ are the grid side currents, $V_{c(a,b,c)}$ are GcC AC side terminal voltages, $i_{c(a,b,c)}$ are the GcC AC side input currents, $S_{(a,b,c)}$ are the GcC switching states, i_{dc} is the GcC DC side output current, i_c is the capacitor current, V_{dc} is the DC-link voltage, i is the DC load (or source) current, C is the DC-link capacitor, L is an inductive filter and R is its internal resistor. P_L and Q_L stand respectively for the active and reactive powers consumed by local loads. The active and reactive powers transferred through the GcC are denoted P and Q, respectively. The ratio between the reactive power generated by the GcC and the one consumed by the local loads is equal to λ. The total active and reactive powers exchanged between the grid and the PCC are denoted P_T and Q_T.

In the following, it is assumed that the d axis is aligned with the grid voltage vector $\underline{V_g}$ and that they have the same phase θ_{dq} (*cf.* Fig.1.b). In this case, the mathematical model of the GcC, expressed in the (d,q) frame, is given by equations (1) and (2) [11].

$$V_{gd} = Ri_{cd} + L\frac{di_{cd}}{dt} - \omega_{dq}Li_{cq} + V_{cd} \tag{1}$$

$$0 = Ri_{cq} + L\frac{di_{cq}}{dt} + \omega_{dq}Li_{cd} + V_{cq} \tag{2}$$

where $\omega_{dq}=d\theta_{dq}/dt$ is the natural frequency of the grid voltage vector $\underline{V_g}$. $V_{g(d,q)}$, $V_{c(d,q)}$ and $i_{c(d,q)}$ are respectively the grid voltages, the GcC AC side terminal voltages and the GcC AC side input currents expressed in the (d,q) frame.

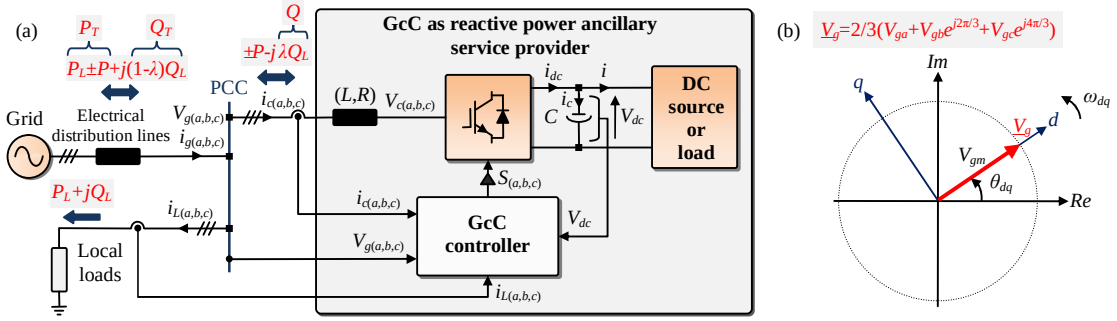

Fig.1. (a) Reactive power ancillary service by three-phase GcC (b) (d,q) synchronous reference frame

The DC-link model can be expressed as follows

$$i_{dc} = i + i_c = i + C\frac{dV_{dc}}{dt} \tag{3}$$

The active and reactive powers (P and Q) drawn through the three-phase GcC are expressed according to equations (4) and (5), respectively [12]. In these equations V_{gm} refers to the peak value of the grid phase voltages.

$$P = \frac{3}{2}V_{gd}i_{cd} = \frac{3}{2}V_{gm}i_{cd} \tag{4}$$

$$Q = -\frac{3}{2}V_{gd}i_{cq} = -\frac{3}{2}V_{gm}i_{cq} \tag{5}$$

According to equations (4) and (5), the control of the active and reactive powers is decoupled: the active power is controlled through the d axis current i_{cd}, while the reactive power is controlled through the q axis current i_{cq}.

2.2. Reactive power ancillary service

As shown in Fig.1.a, the GcC operates with a reactive power ancillary service aimed to compensate an amount $Q=\lambda Q_L$ ($0\leq\lambda\leq1$)) of the reactive power Q_L consumed by local loads. So, assuming that the rated power of the power converter is greater than $\sqrt{(P^2+Q^2)}$, the GcC will operate like a controllable AC current source able to generate a part Q of the whole reactive power Q_L consumed by local loads. The principle of reactive power compensation is depicted on Fig. 2. In this figure, S_i and S_f denote the apparent powers consumed at the PCC before and after reactive power compensation, respectively. The reactive power Q to be injected by the GcC in order to increase the displacement power factor from $\cos(\zeta_i)$ to $\cos(\zeta_f)$ can be deduced according to equation (6.a). Based on this equation, the coefficient λ ($0<\lambda<1$) can be deduced according to equation (6.b).

$$\begin{cases} Q = Q_L - Q_T = P_T(\tan(\zeta_i) - \tan(\zeta_f)) = \lambda Q_L \ (a) \\ \lambda = 1 - (\dfrac{\tan(\zeta_f)}{\tan(\zeta_i)}) \ (b) \end{cases} \quad (6)$$

Notice that the GcC AC side terminal voltage vector can be adjusted in magnitude, frequency and phase via the used GcC controller. So, the reactive power compensation can be adjusted by the GcC AC side input current vector that can be controlled indirectly through modification of the voltage drop on the inductive filter according to the applied GcC AC side terminal voltage vector.

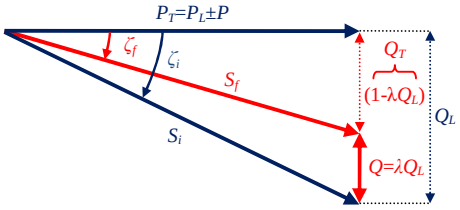

Fig.2. Principle of reactive power ancillary service

2.3. GcC control with reactive power ancillary service

The control of a GcC converter with the ancillay service of reactive power compensation is depicted on Fig.3. This control can be divided into two categories. The first one includes basic control functions, namely : 1) the grid synchronization function [13] that computes the grid voltage phase θ_{dq}, 2) the DC-link voltage controller that controls the DC-link voltage V_{dc} so that it tracks with good accuracy its reference V_{dc}^* [14] and 3) the current controller that controls the grid currents in the (d,q) frame and ensures a decoupled control of the active and reactive powers [15]. The second category includes the ancillary function of reactive power extraction and generation. This function extracts firstly the reactive component of the load current in the (d,q) frame. For this, an *abc-to-dq* coordinate transformation is applied for the measured currents $i_{L(a,b,c)}$ to obtain the load current components in the (d,q) frame $i_{L(d,q)}$. The reactive current is then determined by filtering the i_{Lq} component through a *Low Pass Filter* (LPF). The LPF allows the elimination of harmonic components that may exist in the measured load current when the treated load is a nonlinear load that consumes, besides the reactive current component, an additional harmonic component [16]. Finally, the filtered current i_{Lqf} is multiplied by a constant coefficient λ ($0\leq\lambda\leq1$). This coefficient is selected according to the remaining available power for reactive power ancillary service. The resulting current is imposed at the q axes reference point of the current control loop with an opposite sign ($i_{cq}^*=-\lambda i_{Lqf}$). Thus, the GcC injects a reactive power Q equal to λQ_L.

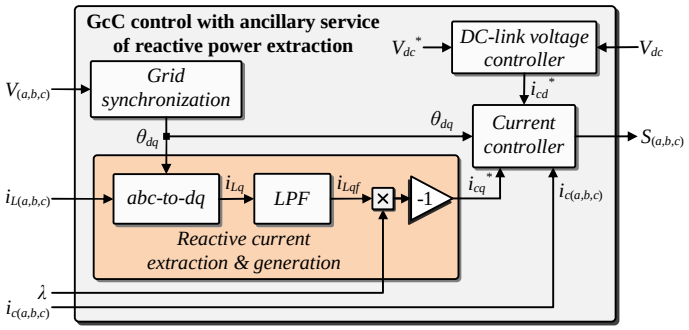

Fig.3. Control of GcC with reactive power ancillary service

3. Technical analysis for minimum required DC-link voltage

The selection of the DC-link voltage level is an important issue for the control of GcCs that operate as reactive power ancillary service providers. In previous publications, there is a lack of research works that investigate on the specification of the minimum required DC-link voltage level for such applications. This paragraph identifies the factors that must be considered for the selection of the DC-link voltage level with detailed analytical expressions that determine the minimum required DC-link voltage value, denoted $V_{dc}^{\min}$. The study is done under both steady-state and transient conditions and is detailed in the following.

3.1. Required minimum DC-link voltage under steady state conditions

The GcC AC side input current vector $\underline{i}_c$, expressed in the complex plane, is the sum of two components $\underline{i}_c^a$ and $\underline{i}_c^r$. The first component ($\underline{i}_c^a$) is the active current, while the second one ($\underline{i}_c^r$) is the reactive current. The magnitude the active and reactive components of $\underline{i}_c$ are supposed equal to I_{cam} and I_{crm}, respectively ($\underline{i}_c=\underline{i}_c^a+\underline{i}_c^r=I_{cam}\cos(\theta_{dq})+jI_{crm}\sin(\theta_{dq})$). Fig.4 shows the phase diagram that characterizes the steady state operation of a GcC with the reactive power ancillary service. Notice that in this figure, the drop voltage across the internal resistor of the inductive filter is neglected.

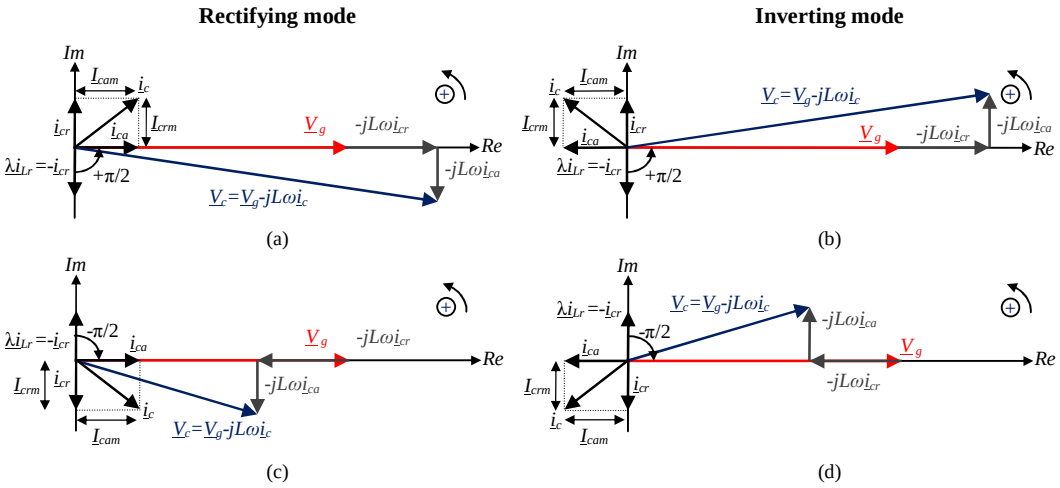

Fig.4. Phase diagram for (a) rectifying mode and leading compensation (b) inverting mode and leading compensation (c) rectifying mode and lagging compensation (d) inverting mode and lagging compensation

Two cases are considered in Fig.4. The first case (Fig.4.a and Fig.4.b) is obtained when the load reactive current lags behind the grid voltage. According to Fig.4.a and Fig.4.b, the amplitude of the GcC AC side terminal voltages under steady-state operation is expressed according to (7) for this first case. As for the second case (Fig.4.c and Fig.4.d), it is obtained when the grid voltage lags behind the load reactive current. Based on Fig.4.c and Fig.4.d, the amplitude of GcC AC side terminal voltages under steady-state operation is expressed according to (8) for the second case.

$$V_{cm}=\sqrt{\left(V_{gm}+L\omega_{dq}I_{crm}\right)^2+\left(L\omega_{dq}I_{cam}\right)^2} \tag{7}$$

$$V_{cm}=\sqrt{\left(V_{gm}-L\omega_{dq}I_{crm}\right)^2+\left(L\omega_{dq}I_{cam}\right)^2} \tag{8}$$

We notice that, in the (d,q) frame, i_{cd} is the active current component, while i_{cq} is the reactive one and the modules of the currents i_{cd} and i_{cq} are respectively equal I_{cam} and I_{crm}. The sign of i_{cd} and i_{cq} depends respectively on the power flow direction (*i.e.* inverting and rectifying modes) and compensation type (*i.e.* leading or lagging compensation) as explained in the following

- When the GcC operates in rectifier mode (*i.e.* the active power is drawn from the AC side to the DC side), the sign of i_{cd} is positive.
- When the GcC operates in inverter mode (*i.e.* the active power is drawn from the DC side to the AC side), the sign of i_{cd} is negative.
- When the reactive power ancillary service compensates an inductive load (*i.e.* leading compensation), the sign of i_{cq} is positive.
- When the reactive power ancillary service compensates a capacitive load (*i.e.* lagging compensation), the sign of i_{cq} is negative.

Thus, equations (7) and (8) can be rearranged in a single equation as follows

$$V_{cm} = \sqrt{\left(V_{gm} + L\omega_{dq} i_{cq}\right)^2 + \left(L\omega_{dq} i_{cd}\right)^2} \tag{9}$$

The minimum required DC-link voltage value $V_{dc}^{\min}$, under steady-state operation, can be deduced according to the following equation

$$V_{dc}^{\min} = \frac{2}{M_{\max}} V_{cm} = \frac{2}{M_{\max}} \left(\left(V_{gm} + L\omega_{dq} i_{cq}\right)^2 + \left(L\omega_{dq} i_{cd}\right)^2\right)^{\frac{1}{2}} \tag{10}$$

where $M_{\max}$ is the maximum value of the modulation index.

For GcCs controlled through a Pulse Width Modulation (PWM) process, the modulation index can reach a maximum value $M_{\max}$ equal to 1. This value can be increased to 1.15, in other words $V_{dc}^{\min}$ decreased by about 15%, if the methods of Space Vector Modulation or third-harmonic injected PWM are used [17]. According to equations (4) and (5), the $i_{c(d,q)}$ currents can be expressed as follows

$$i_{cd} = \frac{P}{1.5V_{gm}} \tag{11}$$

$$i_{cq} = -\frac{Q}{1.5V_{gm}} \tag{12}$$

Substituting equations (11) and (12) in (10), we obtain

$$V_{dc}^{\min} = \frac{2}{M_{\max}} \underbrace{\left(V_{gm}^2 + \left(\frac{L\omega_{dq}}{1.5V_{gm}}\right)^2 \left[P^2 + Q^2\right] - \left(\frac{2L\omega_{dq}}{1.5}\right) Q\right)^{\frac{1}{2}}}_{V_{cm}} \tag{13}$$

The term $L\omega_{dq}$ is generally negligible compared to V_{gm}. Therefore, equation (13) is typically equal to

$$V_{dc}^{\min} \approx \frac{2}{M_{\max}} \underbrace{\left(V_{gm}^2 - \left(\frac{4L\omega_{dq}}{3}\right) Q\right)^{\frac{1}{2}}}_{\approx V_{cm}} \tag{14}$$

Equation (14) shows that, under steady state operation, the minimum required DC-link voltage mainly depends on the amount of the transferred reactive power Q.

3.2. Required minimum DC-link voltage under transient conditions

Neglecting the drop voltage across the internal resistor of the L filter and substituting for $i_{c(d,q)}$ in (1) and (2), from (11) and (12), we obtain the following expression

$$V_{cd} = \frac{L}{1.5V_{gm}} \left(-\frac{dP}{dt} - \omega_{dq} Q\right) + V_{gm} \tag{15}$$

$$V_{cq} = \frac{L}{1.5V_{gm}} \left(\frac{dQ}{dt} - \omega_{dq} P\right) \tag{16}$$

Squaring the left and right sides of equations (15) and (16), adding the resultants and multiplying the square root of the result by ($2/M_{\max}$) yield to equation (17). This equation expresses the minimum required DC-link voltage ($V_{dc}^{\min}$) under both, steady-state and transient conditions.

$$\begin{aligned} V_{dc}^{\min} = \frac{2}{M_{\max}} \underbrace{\sqrt{V_{cd}^2 + V_{cq}^2}}_{V_{cm}} = \frac{2}{M_{\max}} \Bigg\{ & V_{gm}^2 + \left(\frac{L\omega_{dq}}{1.5V_{gm}}\right)^2 \left[P^2 + Q^2\right] - \frac{2L\omega_{dq}}{1.5} Q + \left(\frac{L}{1.5V_{gm}}\right)^2 \left[\left(\frac{dP}{dt}\right)^2 + \left(\frac{dQ}{dt}\right)^2\right] \\ & + \left[2\left(\frac{L}{1.5V_{gm}}\right)^2 \omega_{dq} Q - \frac{2L}{1.5}\right] \frac{dP}{dt} - \left[2\left(\frac{L}{1.5V_{gm}}\right)^2 \omega_{dq} P\right] \frac{dQ}{dt} \Bigg\}^{\frac{1}{2}} \end{aligned} \tag{17}$$

The previous equation shows that the $V_{dc}^{\min}$ voltage can be divided into two components: steady-state and transient components. The steady state component can be deduced based on the steady state values of the active and reactive powers (P and Q), whereas the transient component can be determined based on the time derivatives of the active and reactive powers (*i.e.* dP/dt and dQ/dt). Notice that, during steady state operation, the active and reactive powers (P and Q) are constants. Thus, their time derivatives are equal to zero and equation (17) becomes equal to equation (13), which complies with the steady state analysis (*cf.* paragraph 3.1).

For transient conditions, equation (17) can be simplified to equation (18). This simplification is based on the assumptions that $L<<V_{gm}$, $L\omega_{dq}<<V_{gm}$ and $L^2\omega_{dq}<<V_{gm}^2$.

$$V_{dc}^{\min} \approx \frac{2}{M_{\max}} \underbrace{\sqrt{V_{gm}^2 - \left(\frac{4L\omega_{dq}}{3}\right)Q - \left(\frac{4L}{3}\right)\frac{dP}{dt}}}_{\approx V_{cm}} \tag{18}$$

Compared to equation (16) related to steady-state conditions, equation (18) shows that under dynamic conditions:

- The minimum required DC-link voltage $V_{dc}^{\min}$ is not affected by transient changes of the reactive power Q.
- The minimum required DC-link voltage $V_{dc}^{\min}$ increases when the active power P decreases.
- The minimum required DC-link voltage $V_{dc}^{\min}$ decreases when the active power P increases.

Depending on the value of L and the rise time of the active power, the deviation of $V_{dc}^{\min}$ from its initial value during steady-state conditions to its new value during transient conditions can be significant.

Here, it shall be noticed that the DC-link voltage reference V_{dc}^{*} should be slightly higher than the minimum required DC-link voltage $V_{dc}^{\min}$ to reduce the switching losses and THD of AC side input currents.

3.3. Simulation results

For simulations test, let consider the following case study. The considered system parameters for this case study are depicted on Tab.1.

TABLE I
SIMULATION PARAMETERS

Symbol	Description	value	unit
L	Inductor	10	mH
C	DC bus capacitor	1100	µF
V_{dc}^{*}	DC-link voltage reference value	150	V
V_{gm}	Grid voltage peak magnitude	$100/\sqrt{3}$	V
ω_{dq}	Grid voltage natural frequency	$2\pi 50$	rad/s
$I_{\max}$	Maximum value of the input current i	1.25	A
K_{pdc}	PI proportional gain	0.093	-
k_{idc}	PI integral gain	2.3	-
F_{sw}	Switching frequency	6	kHz

The simulation test scenario related to the considered case study is elaborated for a grid connected rectifier with the following steps. The active and reactive powers (P and Q) are initially equal to zero. Then, at t=0.2s, the active power P changes rapidly from 0 to 187.5W after a sudden 120Ω resistive load connection to the DC-link. After that, at t=0.5s, a step jump from 0 to -2.5A is applied to the i_{cq}^{*} reference current for leading compensation of an amount Q=216.5 VAR of the reactive power. At t=0.8s, the reactive power is again imposed equal to zero by putting the reference i_{cq}^{*} back to zero. At t=1.1s, the reactive power Q is rapidly decreased from 0 to -216.5VAR by setting i_{cq}^{*} to +2.5A for a lagging compensation. At t=1.4s, the reactive power is again imposed equal to zero by putting the reference i_{cq}^{*} back to zero. Finally, at t=1.7s, the active power P is rapidly decreased from 187.5W to 0W by sudden disconnection of the resistive load from the DC-link. Fig.5 shows the obtained simulation results and in Fig.5.a are presented the waveforms of the active and reactive powers related to the considered test scenario. Fig.5.b shows the waveform of the DC-link voltage V_{dc}, which is equal to its reference V_{dc}^{*} during steady state operation. Fluctuations of about 10%V_{dc}^{*} are observed on the DC-link voltage after perturbations caused by sudden connection/disconnection of the resistive load. Conversely, no fluctuations are observed after fast changes of the reactive power transferred by the GcC. This is mainly due to the fact that both of active power and DC-link voltage are controlled through the i_{cd} current component, whereas the reactive power is controlled through the i_{cq} current component. Fig.5.c shows the amount of the minimum required DC-link voltage $V_{dc}^{\min}$, which is deduced by multiplying the amplitude of GcC AC side terminal voltages V_{cm} by 1.15. As predicted by equation (18), fast changes of the active power P is followed by overshoots and undershoots of the $V_{dc}^{\min}$ value. After that, $V_{dc}^{\min}$ reverts to its initial pre-disturbance value. As for the reactive

power, its transient state does not lead to overshoots or undershoots on the V_{dc}^{min} response, but it shifts the V_{dc}^{min} steady state value to a lower (respectively higher) one when a leading (respectively lagging) compensation is achieved. These results are in accordance with the obtained analytical results of equations (14) and (18). It shall be noticed here that, even if it is not true for the considered case study, very large V_{dc}^{min} overshoots and undershoots can be observed when the dynamic of active power change increases. To limit overshoots and undershoots of V_{dc}^{min} during active power transients, the reference current i_{cd}^{*} must be generated gradually. In return, this will affect the control performances, especially for the cases that require fast active power control. On the other hand, as shown in Fig.3, the i_{cd}^{*} is often generated by the DC-link voltage control loop. The dynamic of this control loop is generally very slow compared to that of the internal current control loop [15]. Thus, in practice, the outer DC-link voltage control loop cannot apply step changes for i_{cd}^{*} and active power dynamic will be limited. Also, when no fast control of active power is required, a rate limiter can be added at the DC-link voltage controller output signal to avoid fast changes of the active power and therefore significantly reduces the overshoots and undershoots of V_{dc}^{min}. For the considered case study, the proper operation of the system is ensured since, as shown in Fig.5.b and Fig.5.c, V_{dc}^{min} is always lower than the instantaneous value of the DC-link voltage V_{dc}. Notice that a maximum modulation index M_{max} equal to 1.15 is used for the obtained simulation results. Fig.5.d, Fig.5.e and Fig.5.f illustrate the waveforms of the phase *a* grid current and voltage. It can be noted that no phase delay is perceived between grid current and voltage when the reactive power is equal to zero. However, when the GcC operates as a reactive power provider, the magnitude of the phase *a* current i_{ca} increases and a positive (respectively negative) phase delay is obtained for leading (respectively lagging) reactive power compensation.

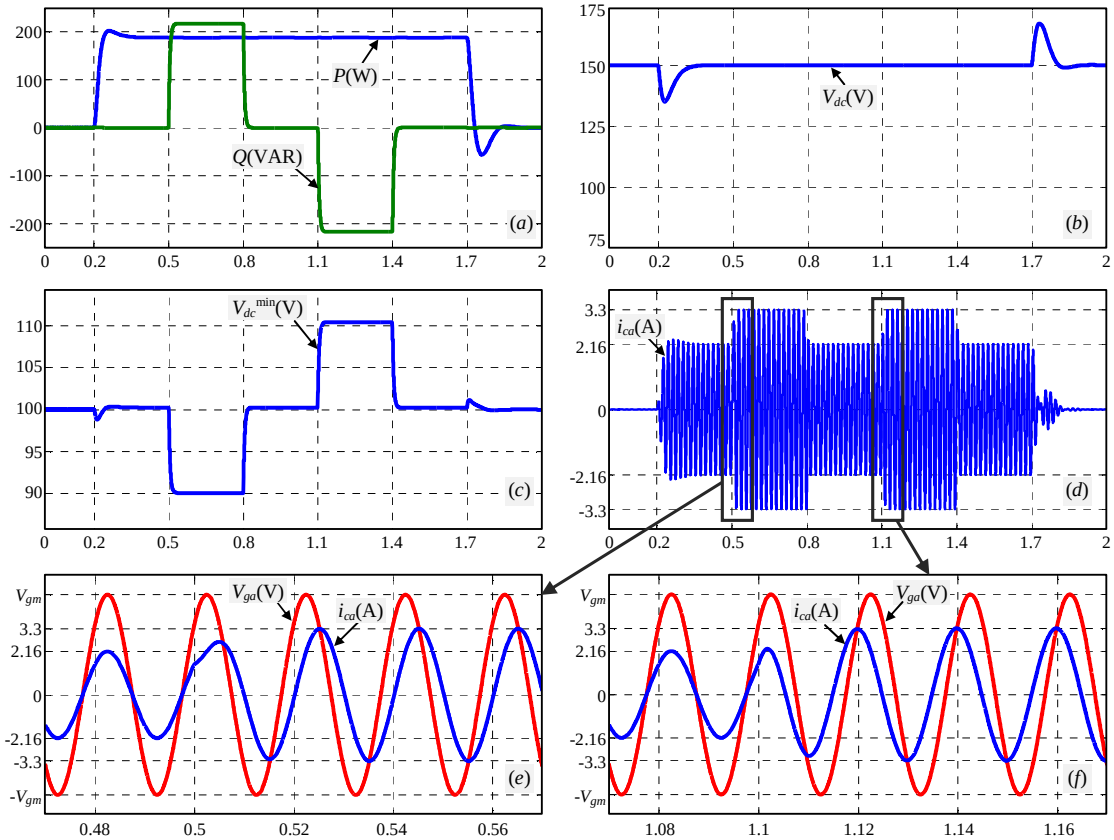

Fig.5. Simulation results (M_{max}=1.15) (a) active and reactive powers (b) DC-link voltage (c) minimum required DC-link voltage (d) phase a grid current (e-f) phase a grid voltage and current under transient conditions

4. Experimental set-up

The experimental tests are done using a three-phase GcC that operates as a rectifier. The developed experimental set-up is depicted on Fig.6 and is composed of three parts. The first one is a power part that consists of an autotransformer, a power converter, three inductive filters (*L*,*R*), a DC-link capacitor *C* and a 120Ω resistive load R_L. The second part is a control part, which is based on the Spartan 6XC6SLX16 FPGA digital solution from Xilinx. This digital solution has a logic cell capability of 2278 Slices (each slice contain four LUTs and eight flip-flops) and is driven through a 100 MHz system clock frequency. Finally, the third part is an interface part that includes the voltages and currents measurement board, analog-to-digital (A/D) and digital-to-analog (D/A)

conversion boards in addition to an interface board that amplifies the power converter switching signals ($S_{(a,b,c)}$) computed by the FPGA from a TTL level to a CMOS level required by the power switches drivers. The experimental tests are done using the same system parameters of Tab.1.

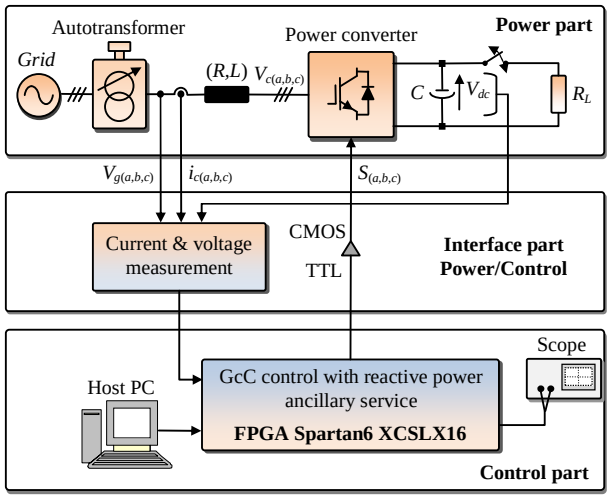

Fig.6. Experimental setup

Fig.7 shows the obtained experimental results after sudden 120Ω resistive load (R_L) connection/disconnection in the DC side. In this case, the response of the DC load current i can be approximated to step changes from 0 to 1.25A (Fig.7.a) and from 1.25A to 0A (Fig.7.b). The step jump of the DC load current i from 0 to 1.25A results in an undershoot, approximately equal to -15V, of the DC-link voltage. After the resistive load connection, the magnitude of GcC AC side input currents increases from 0A to 2.16A. On the contrary, the step jump of the DC load current i from 1.25A to 0A results in an overshoot, approximately equal to +15V, of the DC-link voltage. After the resistive load disconnection, the magnitude of the GcC AC side input currents returns equal to zero.

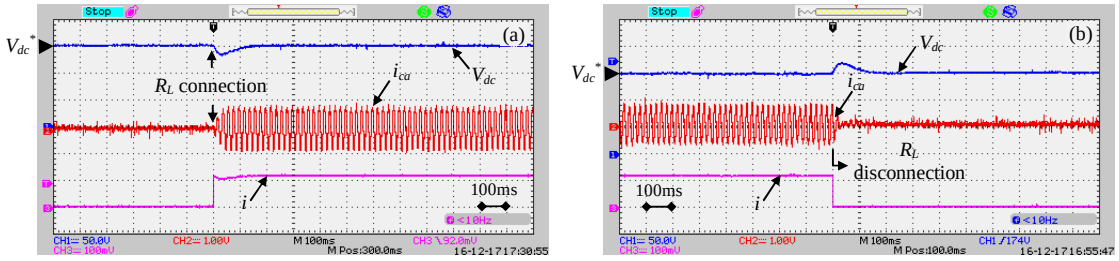

Fig.7. Experimental results of the DC-link voltage V_{dc} (50V/div) and grid current i_{ga} (3.3A/div) and DC load current (1A/div) (a) sudden R_L connection (b) sudden R_L disconnection

Fig.8 shows the obtained experimental results after step jumps equals to ±2.5A applied for the reference current i_{cq}^*. Fig.8 illustrates that, depending on the sign of the reference current i_{cq}^*, leading and lagging reactive power compensation are achieved. We notice here that no deviations are observed on the DC-link voltage after fast changes of the reactive power Q. Fig.8 shows also that, just before the reactive power injection, GcC AC side input current i_{ca} was purely active since there is no phase delay between i_{ca} and V_{ga}. Then, after reactive power injection, a reactive current component is added to the GcC AC side input current i_{ca}. Consequently, its magnitude increases to 3.3A and a phase shift is introduced between the grid voltage V_{ga} and the GcC AC side input current i_{ca}.

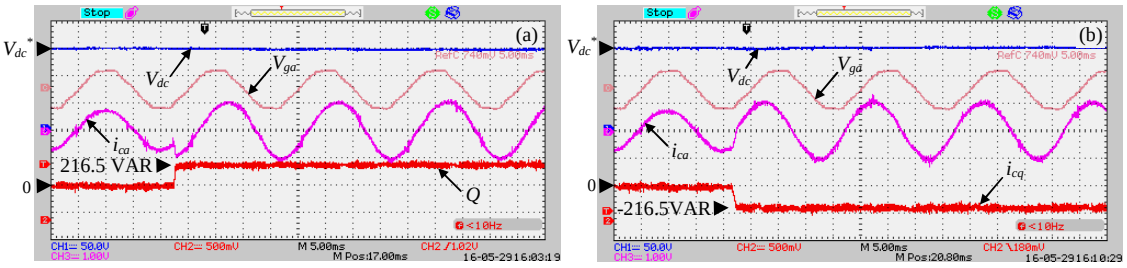

Fig.8. Experimental results of V_{dc} (50V/div), V_{ga} (75V/div), i_{ca} (3.3A/div) and Q (a) step jump of i_{cq}^* from 0A to -2.5A (b) step jump of i_{cq}^* from 0A to 2.5A

5. Conclusion

This paper investigated the benefits of introducing the extra functionality of reactive power provision by three-phase GcC to compensate reactive power consumed by local loads. To ensure proper operation of GcCs with reactive power ancillary service, a detailed analysis regarding the determination of the minimum required DC-link voltage level was achieved. This analyse was done for both steady and transient conditions and for both leading and lagging compensation cases. The obtained mathematical equations show that, during steady state condition, the minimum required DC-link voltage level is primarily dependent on the amount of reactive power. Compared to steady-state conditions, equations obtained for transient conditions reveal that, in addition to the amount of reactive power, the minimum required DC-link voltage depends also on time derivative of the active power P (in others words on the rise time of the active power P). Several simulation and experimental results are presented in order to show the validity of the developed theoretical analysis.

Aknowledgments

"This work was supported by the Tunisian Ministry of High Education and Research under Grant LSE-ENIT-LR11ES15"

References

[1] B. Singh, A. Chandra and K. Al-Haddad, Power quality: problems and mitigation techniques, Wiley ebook, (2015).

[2] A. Kavousi-Frad, A. Khosravi, S. Nahavandi, Reactive power compensation in Electric Arc Furnaces Using Prediction Intervals, IEEE Trans. Ind. Electron. 64 (2017) 5295-5304.

[3] S. Zheng, H. Yan, L. Chen, S. Fang and L. Ge, Research on static VAR generator with direct current control strategy, IEEE Conference on Industrial Electronics and Applications, (2013) 534-537.

[4] Z. Zeng, H. Li, H. Yang, S. Tang, R. Zhao, Objective oriented power quality compensation of multifunctional grid tied inverters and its applications in microgrids, IEEE Trans. Power Electron., 30 (2015) 1255-1265.

[5] N. R. Ullah, K. Bchattacharya, T. Thiringer, Wind farms as reactive power ancillary service providers – technical and economical issues, IEEE Trans. Energy Convers., 24 (2009) 661-672.

[6] M. Prodanovic, K. De Brabandere, J. Van Den Keybus, T. Green, J. Driesen, Harmonic and reactive power compensation as ancillary services in inverter-based distributed generation, IET Generation, Transmission and Ditribution, 1 (2007), 432-438.

[7] N. Jelani, M. Molinas, S. Bolognani, Reactive power ancillary service by constant power loads in distributed ac systems, IEEE Trans. Power Deliv., 28 (2013), 920-927.

[8] M. Molinas, J.Kondoh, Power Electronic Loads as Providers of Reactive Power Ancillary Service to the Grid: Analytical and Experimental study, European Conference on Power Electronics and Applications, (2009), 1-10.

[9] M. P. Kazmierkowski, R. Krishnan, F. Blaabjerg, J. D. Irwin, Control in power electronics : selected problems, Academic press series in engineering, (2002).

[10] G. Zhao, J. Liu, X. Yang, W. Gan, Z. Wang, Analysis and specification of DC side voltage in static var generator regarding compensation characteristics of generators, IEEE Applied power electronic conference and exposition, (2008).

[11] N. Hoffmann, F. W. Fuchs, M. P. Kazmierkowski, D. Schroder, Digital current control in a rotating reference fram – Part I: System modeling and the discrete time-domain current controller with improved decoupling capabilities, 31 (2016), 5290-5305.

[12] M. P. Kazmierkowski, M. Jasinski, G. Wrona, DSP-based control of grid connected power converters operating under grid distortions, IEEE Trans Ind. Informat. 7 (2011) 204-211.

[13] F. Blaabjerg, R. Teodorescu, M. Liserre, A. V. Timbus, Overview of control and grid synchronization for distributed power generation systems, IEEE Trans. Ind. Electron., 53 (2006), 1398–1409.

[14] J. Dannehl, C. Wessels, F. W. Fuchs, Limitations of voltage oriented PI current control of grid connected PWM rectifiers with LCL filters, IEEE Trans. Indus. Electron., 2 (2009), 380-388.

[15] M. Merai, M. W. Naouar, I. Slama-Belkhodja, An improved DC-link voltage control strategy for grid connected converters, IEEE Trans. Power Electron., in press

[16] L. Asiminoael, F. Blaabjerg and S. Hansen, Detection is key – Harmonic detection methods for active power filter applications, IEEE Ind. Appl. Mag, 13 (2007), 22–33.

[17] B. K. Bose, Modern Power Electronics and AC Drives, *Prentice Hall*, (2002).